# A Numerical Simulation of Flow around Rotor Blades Using Overlapped Grid

Akio Ochi*1 and Eiji Shima*1

Takashi Aoyama*2 and Shigeru Saito*2

## Abstract

An unsteady Euler code for rotor blade aerodynamics is developed. A moving overlapped grid method is employed to treat rotating blades. This code has an ability to analyze rotor blade aerodynamic characteristics without modeling wake and tip vortex. Two grid systems are employed to solve the Euler equations. One of the grid systems wraps the rotor blade using boundary fitted coordinates (BFC). The other is the Cartesian background grid covering the whole calculation region including the entire rotor. The calculation is carried out on Numerical Wind Tunnel (NWT) in National Aerospace Laboratory (NAL) to perform large scale and accurate computations. This method is applied for the calculations of hovering and forward flight conditions. The capability of capturing tip vortex is shown by some visualized iso-surfaces of the vorticity magnitude in both cases. In the hover case, the reasonable agreements are obtained between computed and measured pressure distributions on the blade surface and tip-vortex trajectories.

## 1. Introduction

Blade-vortex interaction (BVI) noise is one of the most severe noise problems for helicopters. It is caused by the sudden change of the blade loads during the interactions between the blade and the tip vortices shed from preceding blades. In general, the interactions occur in descending flight conditions, especially during approach to a heliport. The noise generated by the interactions radiates mostly below the helicopter's tip-path plane in the direction of forward flight. The acoustic signal is generally in the frequency range most sensitive to human subjective response (500 to 5000Hz). The BVI noise, therefore, prevents that the commuter helicopter is widely used in the densely populated area.

Wind tunnel experiments for rotorcrafts have technical difficulties because of their complexity for making model rotors and conducting measurements. The techniques of Computational Fluid Dynamics (CFD) help us to understand the detailed flowfield around a rotorcraft. Ahmad et al. [1] performed thin-layer Navier-Stokes calculations including the dynamic motion of a rotor blade using embedded grid method. However more accurate and detailed calculation is required to analyze the BVI phenomenon because, in general, the vortices computed by Euler or Navier-Stokes CFD code are diffused by numerical viscosity. Therefore, more and more grid points are required to capture the tip vortex for the analysis of BVI. As a result, computational costs become too expensive for practical use.

We have developed a new numerical simulation code to analyze the flowfield around rotor blades by solving the Euler equations. A moving overlapped grid method is employed to treat rotating blades. This code uses two grid systems. One of the grid systems wraps the rotor blade using boundary fitted coordinates (BFC). The other is the Cartesian grid covering the whole calculation region including the entire rotor. In this study, we focus on capturing the tip vortex, which strongly affects the BVI phenomenon.

One of the advantages of our code is reducing numerical diffusion. The numerical diffusion is decreased by moving the background grid by the free stream velocity to keep the tip vortex as stationary as possible after projected on the Cartesian background grid. The other advantage is a new fast search and interpolation algorithm to exchange flow data between two grid systems. This algorithm is developed to use vector/parallel computers such as NWT in NAL because a very high performance computer is required to carry out large scale numerical simulations. The CPU time for the search and interpolation is only 5% of the total CPU time for one-blade configuration and 10% for two-blade configuration. In addition, this code will be extended to compute the whole configuration of a rotorcraft, which includes main rotor, fuselage and tail rotor. Our code is easy to apply for such a complex geometry although it is really hard to apply single grid or multi-block grid methods for the comlex geometry.

This report presents some preliminary results to demonstrate the capability of the present CFD code to capture the tip vortex using the moving overlapped grid method. This activity is the first step of our joint study between Advanced Technology Institute of Commuter-helicopter, Ltd. (ATIC) and NAL.

*1 Advanced Technology Institute of Commuter-helicopter, Ltd.
*2 National Aerospace Laboratory

## 2. Calculation method

### 2.1 Numerical schemes

The governing equations of the present simulation are the Euler equations. An inertial force term is included in the calculation of the blade grid. The numerical method[2] to solve the governing equations is an implicit finite-difference scheme. The Euler equations are discretized in the conventional delta form using Euler backward time differencing. A diagonalized ADI method, which utilizes an upwind flux-split technique, is used for the implicit left-hand-side regarding the spatial differencing. In addition, a higher-order upwind scheme based on TVD by Chakravarthy and Osher is applied for the inviscid terms of the explicit right-hand-side. Each ADI operator is decomposed into the product of lower and upper bidiagonal matrices by using diagonally dominant factorization. The TVD scheme has a good capability of capturing the shock wave without adding artificial dissipation. In order to obtain the unsteady solution in the forward flight condition of a helicopter rotor, the Newton iterative method is added. In this method, the above-mentioned scheme

$$LHS(Q^{n+1}-Q^{n})=-\Delta tRHS$$

is modified as

$$LHS^{m}(Q^{m+1}-Q^{m})=-\Delta t(\frac{Q^{m}-Q^{n}}{\Delta t}+RHS^{m})$$

where m means the number of the Newton iteration. The numbers of Newton iteration to reduce the residual at each time-step are 6 and 4 for the blade grid and the background grid, respectively. The typical dividing number along the azimuthal direction is about 3000 per revolution. The unsteady calculation is impulsively started from the azimuth angle of 0 degree. The free stream condition is applied for each of the background-grid boundary.

### 2.2 Grid systems

The moving overlapped grid approach is employed in the present study. Figure 1 shows typical grid systems for one-blade configuration. The density of grid points directly affects the strength of numerical viscosity. The grid spacing near the rotating blade of the Cartesian background grid is about 0.05C for all directions, where C is the cord length of airfoil. The number of grid points is almost 4,500,000 for this grid density. The number of grid points for the blade grid is about 70,000 for each blade. These numbers are not sufficient but compromised for practical use. The size of the calculation region is 8R x 8R x 8R for a forward flight case and 8R x 8R x 12R for a hovering case, where R is the rotor radius. In the hovering case, extra region of 4R in the downward direction is necessary compared with the forward flight case in order to reduce the effect of down wash. The CPU time is 3 hours per revolution by using 26 processing elements of NWT.

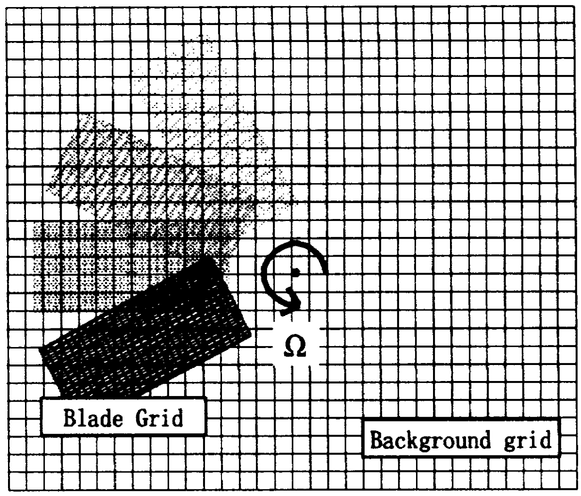


Fig.1 Blade grid and background grid;
Blade grid: 77x 19x 49 = 71687 grid points,
Background grid: 239x239x79 = 4512559 grid points.

### 2.3 Search and interpolation algorithm

The solution vector $Q=(\rho,\rho u,\rho v,\rho w,e)^{t}$ is exchanged between the two grid systems in the moving overlapped grid approach. The search and interpolation to exchange flow data between the two grid systems are executed in each time step because the blade grid rotates with the rotor blade in the background grid.

The computation time spent for search and interpolation is one of the disadvantages of moving grid approach. In our computation, this problem is severe because we use a vector and parallel computer. Thus we have developed a new algorithm, which can be both vectorized and paralellized.

Only the detailed procedure of the data exchange from the blade grid to the background grid is described in this paper because the procedure of the data exchange from the Cartesian background grid to the blade grid is easier than that from the blade grid to the background grid.

The procedure flow of new search and interpolation algorithm is shown in Fig.2. In the first step, the grid indexes (i,j,k) of the background grid point that might be inside of the each blade grid cell are listed. In the second step, the listed indexes are checked whether they are located inside or outside of the grid cell. The position of the point is expressed by three scalar parameters s, t, and u because the tri-linear interpolation is utilized in the present algorithm. In this step, values of s, t, and u for each index are calculated. When all s, t, and u are between zero and one, the point is judged to be located inside of the cell. Figure 3 shows bi-linear interpolation for simplicity. Then the grid points outside of the cell are removed from the list and the flow data are interpolated to temporal arrays. The each processing element (PE) of NWT performs these procedures in parallel. Finally, the interpolated values are exchanged between the processing elements.

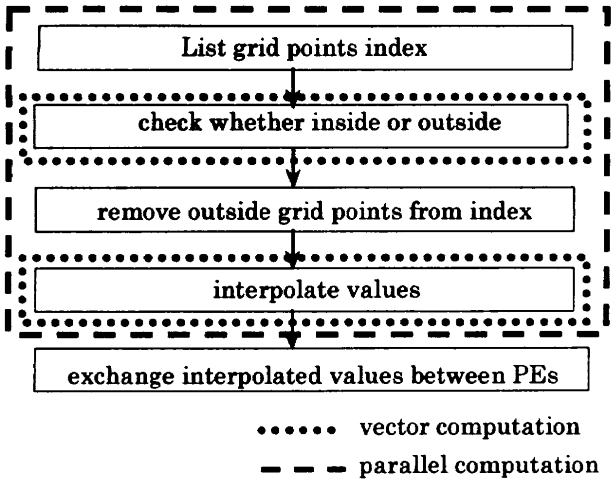


Fig.2 Procedure flow of search and interpolation.

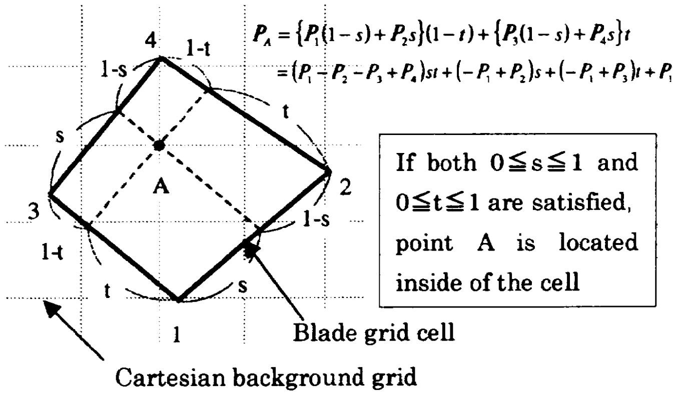


Fig.3 Bi-linear interpolation.

## 4. Results and discussions

The comparisons of computed and measured[3] pressure coefficient distributions for hovering conditions are shown in Figs.4 and 5. The detailed test conditions are shown in Table 1. The tip Mach number for Figs.4 and 5 are transonic ($M_{tip}$=0.877) and subsonic ($M_{tip}$=0.439), respectively. The agreement between computed and measured results is quite good in the transonic case although disagreement is observed at the inner stations in the subsonic case.

Figure 6 shows the typical trajectory of the tip vortex in a hovering condition. The tip vortex descends with contracting. It is very important to obtain the accurate location of tip vortex to make an analysis of BVI because the intensity of BVI depends on the relative position between rotor blade and the tip vortex. The comparisons of computed and measured positions of the tip vortex are shown in Fig.7. The agreement between the computed and measured displacements is quit good in the transonic case although it is not enough in the subsonic case. This result might be caused by the overestimation of the lift shown in Fig.5. The computed contractions are in good agreement with the results of Kocurek's formula although they overestimate the experimental data both in the transonic and the subsonic cases. The tip vortices are visualized by the iso-surfaces of vorticity magnitude in Fig.8. The tip vortices can be captured almost one revolution although the diffusion by numerical viscosity is observed.

Figures 9a)~i) show visualized tip vortices at different azimuth angles in the forward flight condition shown in Table 1. The tip vortices are clearly captured also in this condition. The tip vortices generated at the advancing side are much stronger than those generated at the retreating side because the flapping and the feathering motions of the blade are not included in this calculation. The present code is now being extended in order to be applied for the calculation including these motions. The validation in the forward flight condition is not completed at present because instability of calculation is observed at the retreating side especially in the case of high advance ratio.

## 5. Conclusions

An unsteady Euler code for rotor blade aerodynamics is developed. A moving overlapped grid method is employed to treat rotating rotor blades. The capability of capturing tip vortex is shown by some visualized iso-surfaces of the vorticity magnitude in hover and forward flight. In the hover case, the agreement between computed and measured pressure distributions on the blade surface is quite good in transonic case although disagreement is observed at the inner stations in the subsonic case. The agreement between the computed and measured displacements of tip vortex is quit good in the transonic case although it is not enough in the subsonic case. The computed contractions are in good agreement with the results of Kocurek's formula although they overestimate the experimental data both in the transonic and the subsonic cases.

## References

[1] Ahmad,J and Duque,E.P.N., Helicopter Rotor Blade Computation in Unsteady Flows Using Moving Embedded Grids, AIAA Paper 94-1922, June 1994.

[2] Aoyama,T., Kawachi,K., and Saito,S., Unsteady Calculation for Flowfield of Helicopter Rotor with Various Tip Shapes, 18th European Rotorcraft Forum, Paper No.B03, Avignon, France, September 1992.

[3] Caradonna,F.X. and Tung,C., Experimental and Analytical studies of a Model Helicopter Rotor in Hover," 6th European Rotorcraft and Powered Lift Aircraft Forum, Paper No.25, Bristol, England, September 1980.

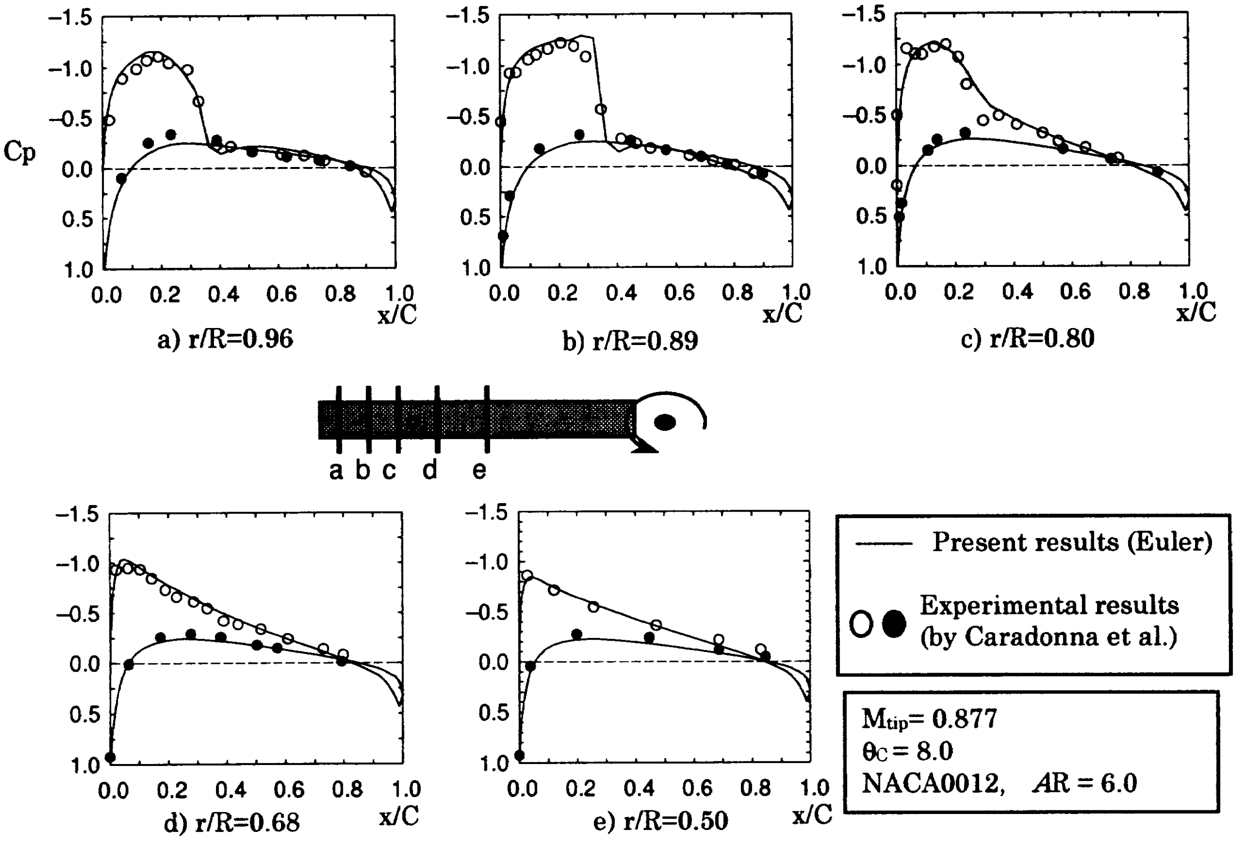


Fig.4 Comparison of computed and mesured pressure coefficient distributions in transonic hover case.

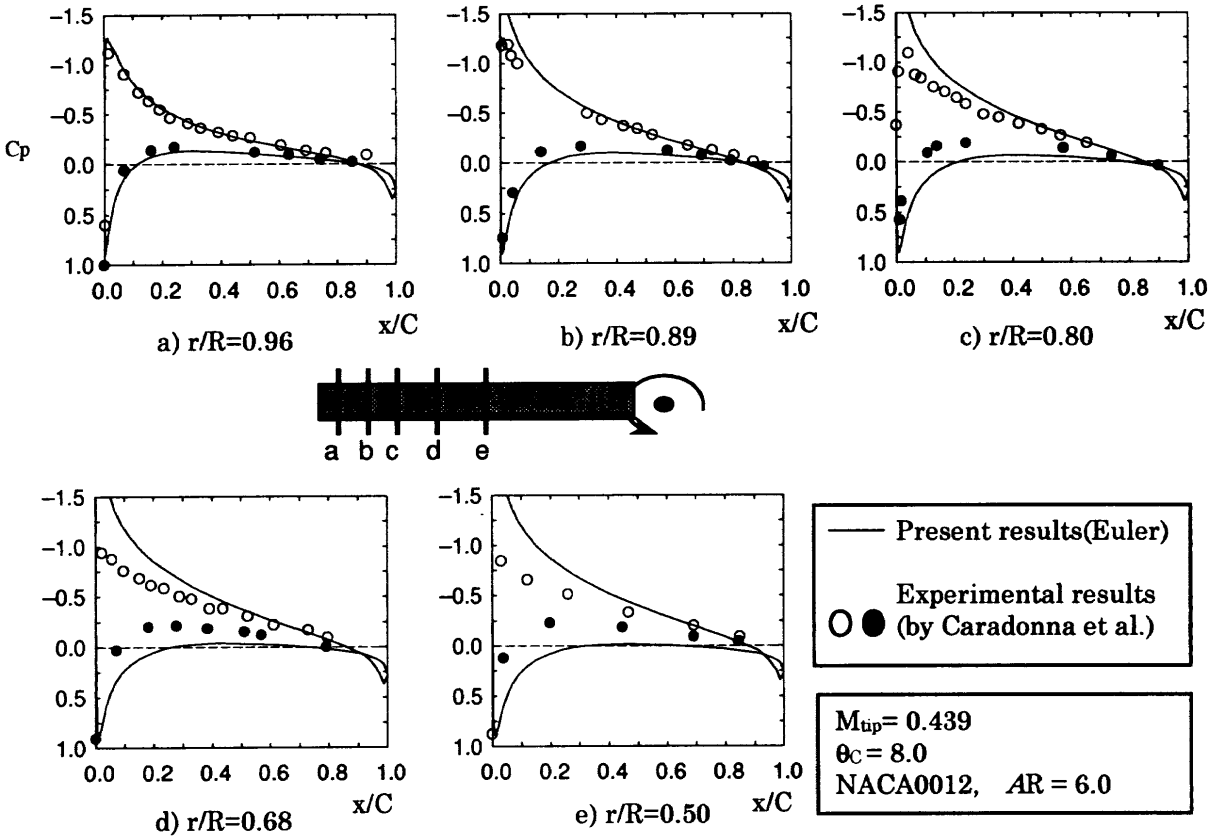


Fig.5 Comparison of computed and mesured pressure coefficient distributions in subsonic hover case.

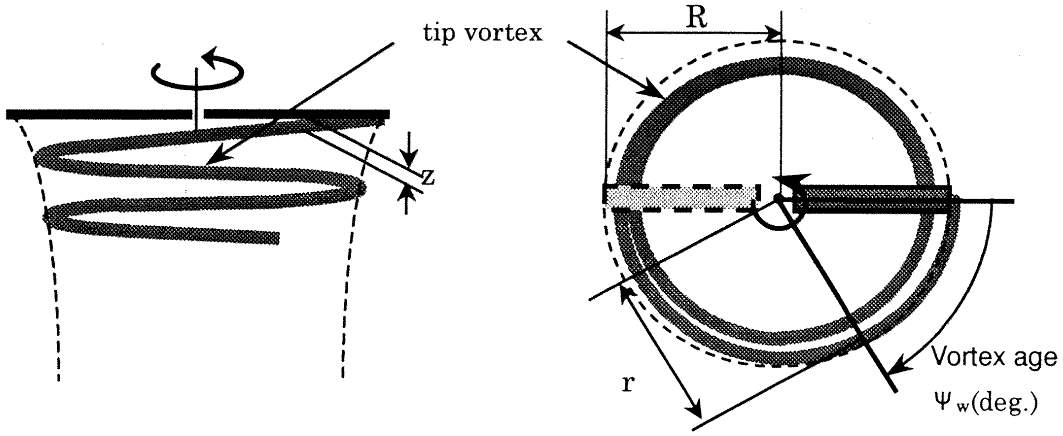


a) Displacement

b) Contraction

Fig.6 Typical trajectory of tip vortex in hover.

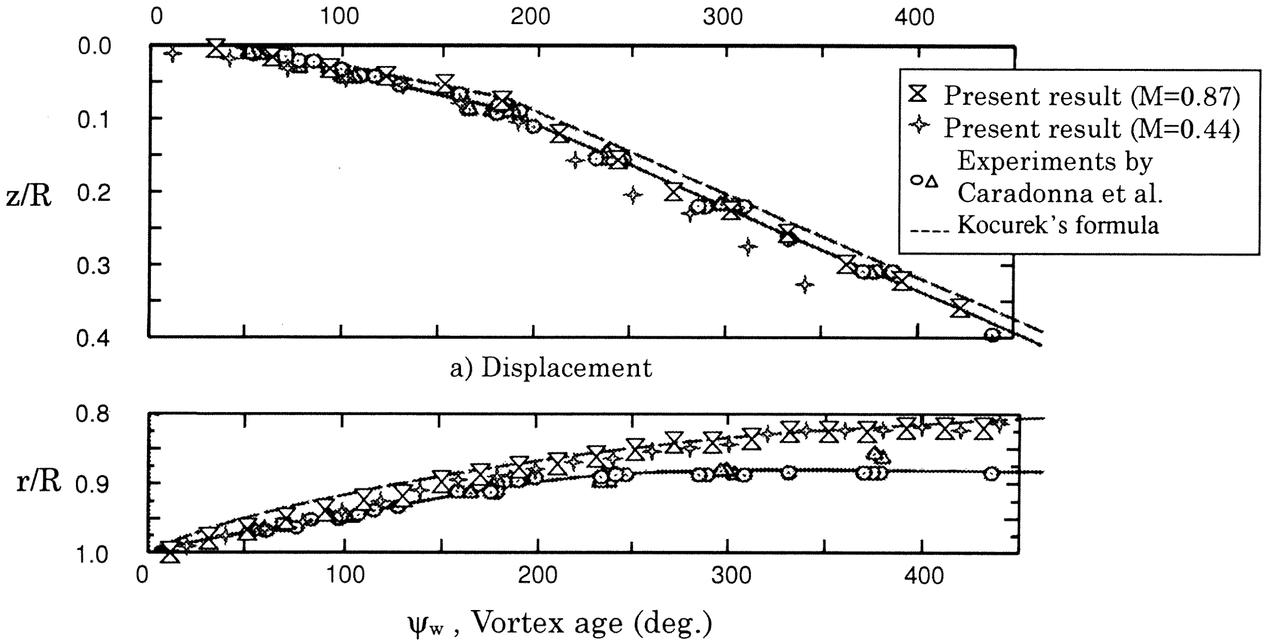


b) Contraction

Fig.7 Comparison of computed and measured position of tip vortex.

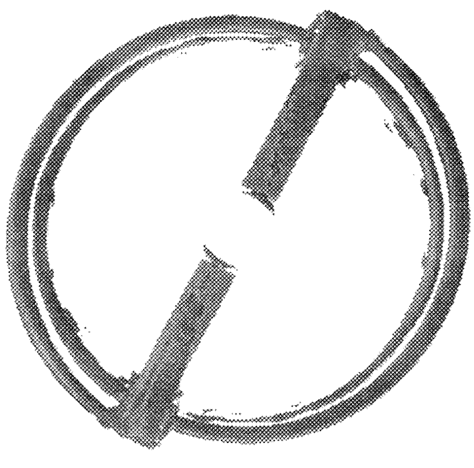

Fig.8 Visualized tip vortices in hover (iso-surface of vorticity magnitude).

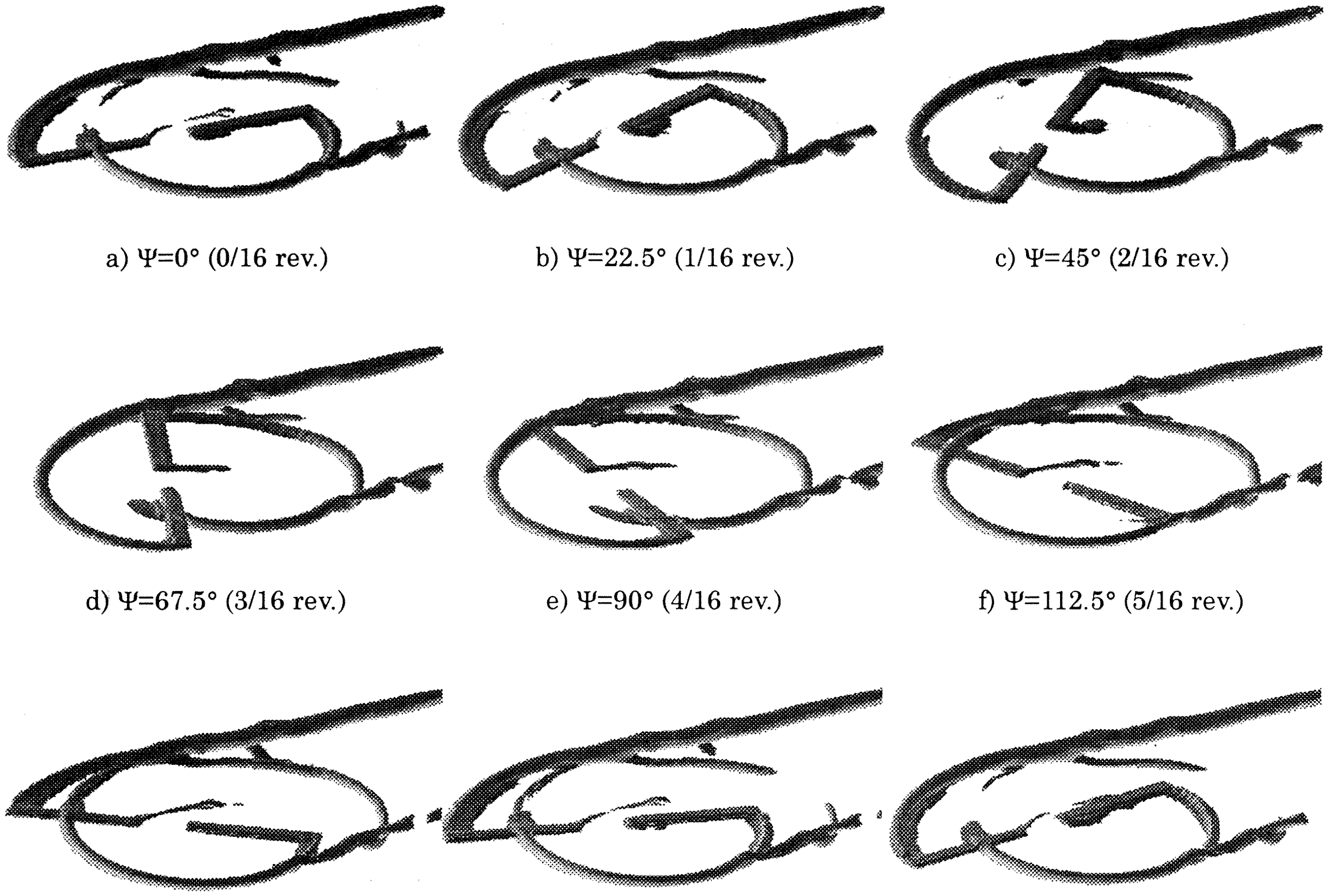

a) Ψ=0° (0/16 rev.) b) Ψ=22.5° (1/16 rev.) c) Ψ=45° (2/16 rev.)

d) Ψ=67.5° (3/16 rev.) e) Ψ=90° (4/16 rev.) f) Ψ=112.5° (5/16 rev.)

g) Ψ=135° (6/16 rev.) h) Ψ=157.5° (7/16 rev.) i) Ψ=180° (8/16 rev.)

Fig.9 Visualized tip vortices in forward flight.

Table 1 Calculation conditions.

| Condition | Hover | Forward flight |
|---|---|---|
| Aspect ratio | 6.0 | 8.33 |
| Number of blade | 2 | 2 |
| Airfoil | NACA0012 | NACA0012-64 |
| Tip planform | rectangular | rectangular |
| Hover tip Mach number | 0.439 / 0.877 | 0.4312 |
| Forward flight Mach number | 0 | 0.0688 |
| Collective pitch angle | 8.0° | 6.0° |
| Cyclic pitch angle | 0 | 0 |
| Number of Grid points for each blade | 131,747 | 119,475 |
| Number of Grid points for background | 4,774,109 | 4,836,825 |